MECHANISM OF ADSORPTION OF CATIONS ONTO ROCKS

A. KITAMURA [1], K. FUJIWARA [2], T. YAMAMOTO [1],
S. NISHIKAWA [3] and H. MORIYAMA [3]

[1] Department of Nuclear Engineering, Osaka University,
Yamadaoka, Suita, Osaka, 565-0871, Japan
[2] Department of Nuclear Engineering, Kyoto University,
Yoshida-Honcho, Sakyo-ku, Kyoto, 606-8501, Japan
[3] Research Reactor Institute, Kyoto University,
Noda, Kumatori-cho, Sennan-gun, Osaka, 590-0494, Japan

ABSTRACT

Adsorption behavior of cations onto granite was investigated. The distribution coefficient (K_d) of Sr^{2+} and Ba^{2+} onto granite was determined in the solution of which pH was ranged from 3.5 to 11.3 and ionic strength was set at 10^{-2} and 10^{-1}. The K_d values were found to increase with increasing pH and with decreasing ionic strength. The obtained data were successfully analyzed by applying an electrical double layer model. The optimum parameter values of the double layer electrostatics and adsorption reactions were obtained, and the mechanism of adsorption of cations onto granite was discussed. Feldspar was found to play an important role in their adsorption.

INTRODUCTION

Understanding of radionuclide migration behavior is important for the safety assessment of geologic disposal of radioactive wastes. Extensive studies have been performed to obtain the data of adsorption of various radionuclides onto solids and rocks. However, the experimental adsorption data are usually described by empirical means, including distribution coefficients and isotherm equations. These empirical relationships and parameters are highly dependent on the chemical conditions of the experimental system and are considered unsatisfactory from a scientific point of view. A thorough and mechanistic understanding of the adsorption-desorption reactions is needed for understanding and predicting their role in the migration behavior of radionuclides [1, 2].

There are many studies dealing with a solid-liquid interface by using an electrical double layer model [3, 4]. In the model, it is assumed that the adsorbent surface has specific acid-base characters due to hydrolysis. This approach has been coupled with suitable speciation models for chemical species in computer codes and has been successfully applied to describe the equilibrium distributions of some radionuclides at a solid-liquid interface, e.g., between groundwater and mineral surface [5-7]. Because of its usefulness, the model may be

applied to the other adsorption systems and improved as required [8].

In our previous study, the adsorption behavior of various cations onto quartz was discussed [9]. The measured distribution coefficients and surface charge densities were successfully analyzed by using the electrical double layer model, and optimum parameter values were obtained. It was found that the parameter values for the electrostatic capacitance and then the dielectric constant in the electrical double layer are much dependent on the distance from the surface because of electrical saturation of water molecules near the surface. Also, the intrinsic adsorption equilibrium constants of the adsorbate cations were found to be simply related with the Coulomb potential differences resulting from their adsorption.

The present study is an extension of our previous study and deals with the adsorption behavior of various cations onto granite. Granite is noted as one of the bedrocks proposed for a disposal site of radioactive wastes. In this study, the distribution coefficient of Sr^{2+} and Ba^{2+} onto granite was determined by a batch method, and the pH and ionic strength dependencies of the obtained data were analyzed by the model of Davis et al. [3, 10]. Together with the results for Cs^{+} [11] and Am^{3+} [12], the optimum parameter values of double layer electrostatics and intrinsic adsorption equilibrium constants for Sr^{2+} and Ba^{2+} were discussed for some details of the adsorption mechanism.

EXPERIMENTAL

Distribution coefficient (K_d) of Sr^{2+} and Ba^{2+} onto granite was determined by a batch method. The granite sample was a biotite granite obtained from Inada, Ibaraki, Japan (Nichika Co). The granite sample was crushed to the mesh size of 32~60 and washed with 0.5 mol dm^{-3} HCl. The specific surface area was determined to be 0.11 $m^2 g^{-1}$ by a BET method. In a polypropylene tube, 0.1 g of granite powder was added into 4.0 ml of $NaClO_4$ solution. The electrolyte concentration was set at 10^{-2} mol dm^{-3} or 10^{-1} mol dm^{-3}. The initial concentration of Sr^{2+} or Ba^{2+} in the solution was 2.0×10^{-4} mol dm^{-3}. The pH of the solution was adjusted by either $HClO_4$ or NaOH. The sample was gently contacted with shaking for 7 days at 24±3 °C to attain adsorption equilibrium. After centrifugation at 3,000 rpm for 10 min, the pH values were determined by using a pH meter, HM-30V (TOA Electronics Co.), and the concentration of Sr^{2+} or Ba^{2+} in the solution was measured by inductively coupled plasma atomic emission spectroscopy, ICPS-1000TR (Shimadzu Co.). The experiments were performed in a glove box filled with argon to avoid the contamination and complexation by carbonate.

RESULTS AND DISCUSSION

Distribution Coefficient

The K_d (ml g^{-1}) value was calculated by the following equation :

$$K_d = \frac{([M^{z+}]_0 - [M^{z+}]_f)V}{[M^{z+}]_f W}, \quad (1)$$

where $[M^{z+}]_0$ (mol dm^{-3}) and $[M^{z+}]_f$ (mol dm^{-3}) denote the concentrations of the adsorbate ion before and after equilibration, respectively, V (ml) the volume of the solutions and W (g) the weight of the dried granite sample.

The obtained K_d values of Sr^{2+} and Ba^{2+} are shown as a function of pH in Figures 1 and 2, respectively. As seen in these figures, the K_d values increase with increasing pH and with decreasing ionic strength of the electrolyte solution.

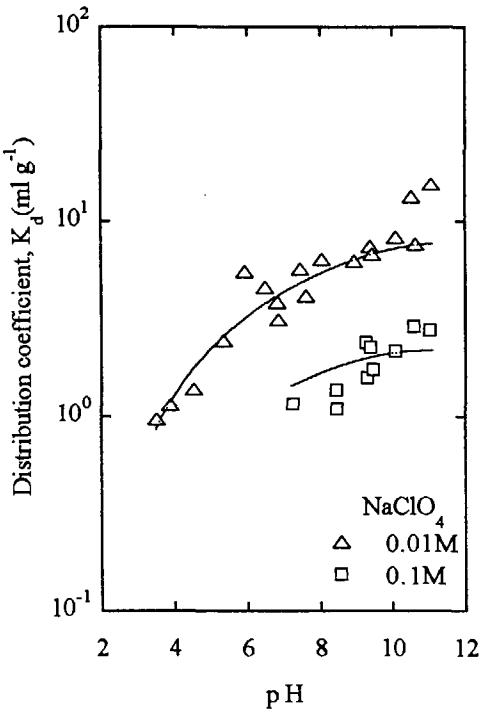

Fig. 1 Distribution coefficient of Sr^{2+} onto granite. Marks are experimental and curves represent the least-squares fit of the experimental data to the electrical double layer model.

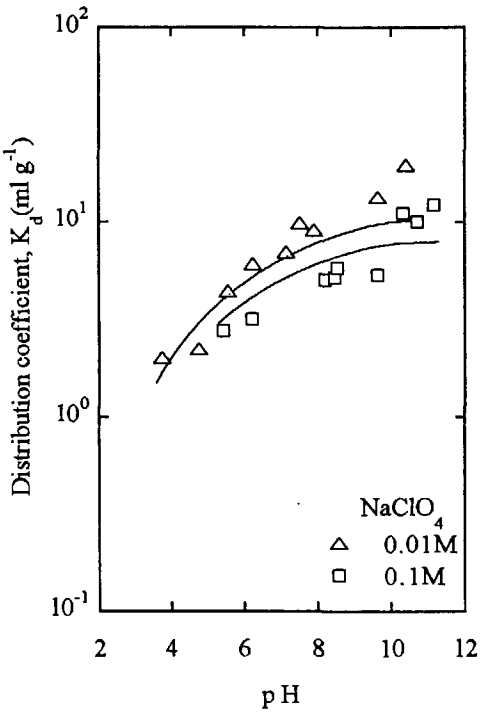

Fig. 2 Distribution coefficient of Ba^{2+} onto granite. Marks are experimental and curves represent the least-squares fit of the experimental data to the electircal double layer model.

Electrical Double Layer Model

Granite is composed of many mineral components, and different kinds of adsorption sites are expected to be present at the surface of granite. In the present study, however, any adsorption sites in the mineral components are represented by SOH for simplicity. The hydroxylated surface is mainly responsible for the surface charge as

$$SOH_2^+ \rightleftarrows SOH + H_s^+ \quad (2)$$
$$SOH \rightleftarrows SO^- + H_s^+ \quad (3)$$

where S denotes the metal ions at the mineral surface, K_{a1}^{int}, K_{a2}^{int} are the intrinsic acidity constants of reactions (2) and (3), respectively, and the subscript s denotes the surface. In the present study, the adsorption of anions is assumed to be negligibly small in the case of mineral components of granite considering that the points of zero charge are around 2 - 4 [13, 14]. Similarly to the case of quartz [14], the adsorption data of cations onto granite are analyzed by the electrical double layer model of Davis et al. [3, 10]

In their model, it is assumed that the adsorbent surface has specific acid-base characteristics, and that the adsorbate ion is subject to the double layer electrostatics. In addition to the diffuse layer, the compact Stern layer is composed of an inner layer and an outer layer with their own electrostatic capacitances, C_1 and C_2, respectively. Together with reaction (3), the following surface reactions for cations (M^{z+}) is considered in the present study :

$$SO^- + Na_\beta^+ \rightleftarrows SO^-\text{-}Na^+ \quad (4)$$
$$SO^- + M_\beta^{z+} \rightleftarrows SO^-\text{-}M^{z+} \quad (5)$$

where the subscript β denotes the plane of counter ions closest to the surface, i.e., the Helmholtz plane. Reactions (4) and (5) may compete with each other in equilibrium at the present system. Equations used in the analysis are thus given as follows [9]:

$$K_{a2}^{int} = \frac{[SO^-][H^+]_b}{[SOH]} \exp\left(\frac{-e\psi_s}{kT}\right) \quad (6)$$
$$K_{Na}^{int} = \frac{[SO^-\text{-}Na^+]}{[SO^-][Na^+]_b} \exp\left(\frac{e\psi_\beta}{kT}\right) \quad (7)$$
$$K_M^{int} = \frac{[SO^-\text{-}M^{z+}]}{[SO^-][M^{z+}]_b} \exp\left(\frac{ze\psi_\beta}{kT}\right) \quad (8)$$
$$N_s = B([SOH]+[SO^-]+[SO^-\text{-}Na^+]+[SO^-\text{-}M^{z+}]) \quad (9)$$
$$\sigma_s = -B([SO^-]+[SO^-\text{-}Na^+]+[SO^-\text{-}M^{z+}]) \quad (10)$$
$$\sigma_\beta = B([SO^-\text{-}Na^+]+ z[SO^-\text{-}M^{z+}]) \quad (11)$$
$$\sigma_d(Na) = -0.1174\sqrt{c}\sinh\left(\frac{e\psi_d}{2kT}\right) \quad (12)$$
$$\sigma_d(M) = (z\,[M^{z+}]_b / [Na^+]_b)\,\sigma_d(Na) \quad (13)$$
$$\sigma_s + \sigma_\beta + \sigma_d(Na) + \sigma_d(M) = 0 \quad (14)$$
$$\psi_s - \psi_\beta = \sigma_s / C_1 \quad (15)$$
$$\psi_\beta - \psi_d = -\sigma_d / C_2 \quad (16)$$
$$B = 10^{-3} FV / S_0 W \quad (17)$$
$$K_d = 10^3\, S_0 \times \frac{B[SO^-\text{-}M^{z+}] + \sigma_d(M)}{N_A e[M^{z+}]_b}, \quad (18)$$

where K_{Na}^{int} and K_M^{int} are the intrinsic constants of local equilibrium reactions (4) and (5), respectively, z the number of charge, e the electronic charge (1.60×10^{-19} C), ψ the variable electrostatic potential in the double layer, k the Boltzmann constant (1.38×10^{-23} J K^{-1}), T the absolute temperature (K), N_s the surface site density (C m^{-2}), σ the charge density (C m^{-2}), c the electrolyte concentration (M), B the conversion factor from mol dm^{-3} to C m^{-2}, F the Faraday constant (9.65×10^4 C mol^{-1}), V the liquid volume (m^3), S_0 the surface area (m^2 g^{-1}), N_A the Avogadro number (6.02×10^{23} mol^{-1}), and the subscripts b and d denote the bulk and the diffuse layer, respectively. For the variable electrostatic potential in the electrical double layer, the concentration of each species X in the layer can be related to its bulk solution concentration by the Boltzmann factor as given by $[X]_i = [X]_b \exp(-ze\psi_i / kT)$, where i=s, β or d. The K_d value which is experimentally determined are obtained by equation (18) from the surface charge density.

Not only the ions existing in the compact Stern layer but also those in the diffuse layer should be regarded as adsorbed ions as observed for Na^+ ions [15]. The contribution of M^{z+} in the diffuse layer is thus assumed to be expressed by equation (13) [9]. In the present case, however, the contribution of the adsorbate ions in the diffuse layer to the measured distribution coefficient has been found to be negligibly small since the concentration ratio of $[M^{z+}]/[Na^+]$ in the diffuse layer is as small as that in the bulk solution. Only the contribution of the adsorbate ions in the compact Stern layer is important in the present analysis.

Obtained Parameter Values

In the model, a number of parameters are contained in the equations. Those are N_s, K_{a2}^{int}, C_1, C_2, K_{Na}^{int} and K_M^{int}. Some of the parameters may be considered to compete with each other, and it is necessary to reduce the number of free parameters for a proper convergence. In the analysis, the surface site density of 5 sites nm^{-2} for silica [16] was assumed because of the lack of data for other mineral components, and the C_2 value of 0.20 F m^{-2} was also assumed which was used in several literatures [1-4, 17-19]. In the previous study of Am^{3+}, the surface area S_0 was treated as one of free parameters and found to be almost the same as the value of 0.11 m^2 s^{-1} measured by a BET method [12]. Then the surface area S_0 was set at 0.11 m^2 s^{-1} in the present analysis. The intrinsic acidity constant, K_{a2}^{int}, was derived from the titration data for quartz (log K_{a2}^{int} = -6.57), microcline as a representative of feldspars (-2.12) and biotite (-11.9) [11].

The obtained parameter values are summarized in Table 1, where the χ^2 value denotes a variance between the experimental and calculated values. In the analysis of the data for granite, only the calculation using K_{a2}^{int} = -2.12 has properly converged for the analysis of Cs^+, Sr^{2+} and Ba^{2+}, and the K_{a2}^{int} = -3.6 ± 0.6 was obtained in the analysis of Am^{3+} [12]. It follows that these ions may be mainly adsorbed onto feldspar of granite.

The results of the least squares fittings of the experimental data are shown as curves in Figures 1 and 2. It can be seen that the pH and ionic strength dependencies of the experimental data are reasonably described by the model.

Table 1 Optimum parameter values derived from the least-squares fit of the K_d values of Cs^+, Sr^{2+}, Ba^{2+} and Am^{3+} for granite to the electrical double layer model.

adsorbate ions	Cs^{+} 1)	Sr^{2+}	Ba^{2+}	Am^{3+} 2)
C_1 (F m^{-2})	0.19 ± 0.01	2.43 ± 0.49	2.64 ± 0.81	0.06 ± 0.03
log K_{a2}^{int}	-2.12 3)	-2.12 3)	-2.12 3)	-3.6 ± 0.6
log K_{Na}^{int}	0.72 ± 0.16	-0.21 ± 0.29	-0.96 ± 0.54	-0.6
log K_M^{int}	5.41 ± 0.15	0.23 ± 0.59	0.78 ± 1.11	4.8 ± 1.0
χ^2	0.108	0.390	0.284	1.21

1) The data in Ref. [11] were reanalyzed by using the S_0 value of 0.11 m^2 g^{-1}.
2) Ref. [12].
3) The K_{a2}^{int} value of $10^{-2.12}$ determined for the Na^+ adsorption onto microcline was used in the analysis [11]. See text for details.

There are some differences between the experimental and calculated values at higher pH values. Around pH 10, the calculated values show some saturation behaviors possibly because of saturated surface charge density of feldspars while the experimental values still increase. This difference may be explained by considering additional contribution of biotite of which the content is expected to be a few percent in the granite [20]. The K_{a2}^{int} of biotite is known to be $10^{-11.9}$, and then its surface charge density increases in this pH region. For more detailed analysis, such a two-site model may be required.

Relationship between the Electrostatic Capacitance and Dielectric Constant

The electrostatic capacitance C_1 per unit area (F m^{-2}) is given as

$$C_1 = \varepsilon_0 \varepsilon_1 / d_1 , \qquad (19)$$

where d_1 (m) denotes the distance between the adsorbent surface and the Helmholtz plane, ε_0 the vacuum permittivity (8.854×10^{-12} F m^{-1}) and ε_1 the relative dielectric constant. As shown in Figure 3, the ε_1 values have been evaluated by taking the Stokes radii for d_1 in our previous study [9]. It was found that the ε_1 values decrease with decreasing distance from the surface because of the electrical saturation of water molecules near the surface as suggested by Grahame [21]. A similar situation is found to hold for the presently obtained ε_1 values in the case of Sr^{2+} and Ba^{2+} for granite. Then it is considered that these cations are adsorbed onto the mineral surface in the form of fully hydrated ions.

In the case of Cs^+ and Am^{3+} of which the concentrations are much lower than those of

Na^+ as an ionic strength controlling agent, on the other hand, the obtained ε_1 values are found to be much smaller than those for Sr^{2+} and Ba^{2+}. Following our previous study [9], a possible explanation may be given by considering very low concentration of adsorbate cations and by considering the effect of heterogeneous surface structures on the ε_1 values. There may be a variety of the surface structures resulting in different ε_1 values and some of the surface structures may be very effective for adsorption with smaller ε_1 values. In the case of the K_d determination, the concentration of the adsorbate cations of interest is usually much lower than that of Na^+ and the adsorbate ions are preferably adsorbed on the surface of smaller ε_1 values.

Intrinsic Adsorption Equilibrium Constants

In our previous study [9], the log K_M^{int} values were found to be related with the difference in the Coulomb potentials, ΔE_c, between the adsorbate ions at the Helmholtz plane and those at the start of the diffuse layer, which is given by

$$\Delta E_c = \frac{aZ_M e^2}{\varepsilon_0 \varepsilon_1 d_1} - \frac{aZ_M e^2}{\varepsilon_0 \varepsilon' d'} = \frac{aZ_M e^2}{C_1 d_1} - \frac{aZ_M e^2}{C' d'} , \quad (20)$$

where a denotes a constant, Z_M the valence of the adsorbate ions, C' (F m^{-2}) and d' (m) the capacitance and the distance between the surface and the start of the diffuse layer, respectively. Considering that the compact Stern layer is composed of an inner layer and an outer layer with their own electrostatic capacitances, C_1 and C_2, respectively, the C' and d' values are obtained by

$$\frac{1}{C'} = \frac{1}{C_1} + \frac{1}{C_2} \quad (21)$$

$$d' = d_1 + d_2 \quad (22)$$

$$d_2 = \varepsilon_0 \varepsilon_2 / C_2 , \quad (23)$$

where d_2 (m) and ε_2 denote the distance and relative dielectric constant between the Helmholtz plane and the start of the diffuse layer, respectively. In the calculation, the ε_2 value is assumed to be of water, that is 78.5.

Figure 4 shows the log K_M^{int} values as a function of ΔE_c. As shown by dashed line, a simple relationship may be found not only for quartz but also for feldspar in granite. Thus it is concluded that no particular difference exists in the adsorption mechanisms between both adsorbents. This kind of relationship is useful not only for checking the experimental data but also for predicting the unknown values since the ΔE_c values are estimated from the Stokes radii and the C_1 values which are easily obtained from the ε_1 values following such a relationship shown in Figure 3.

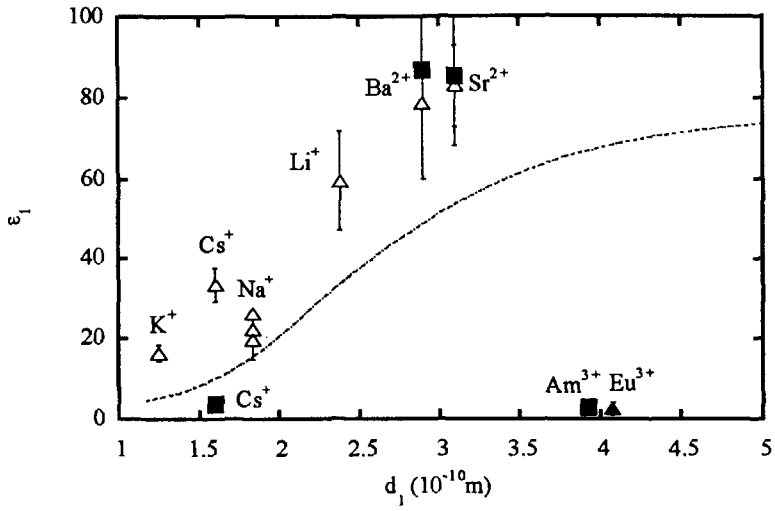

Fig. 3 Relative dielectric constant ε_1 as a function of the distance d_1 between the mineral surface and the center of cations. Marks are the analytical data of titration experiment for quartz (△), of K_d measurement for quartz (▲) and of K_d meausrement for granite (■). Dashed curve represents the relative dielectric constant of water as a function of d_1 [21]. The crystal ionic radius of Cs^+ (1.67×10^{-10} m) is used for d_1 instead of the Stokes radius (1.16×10^{-10} m).

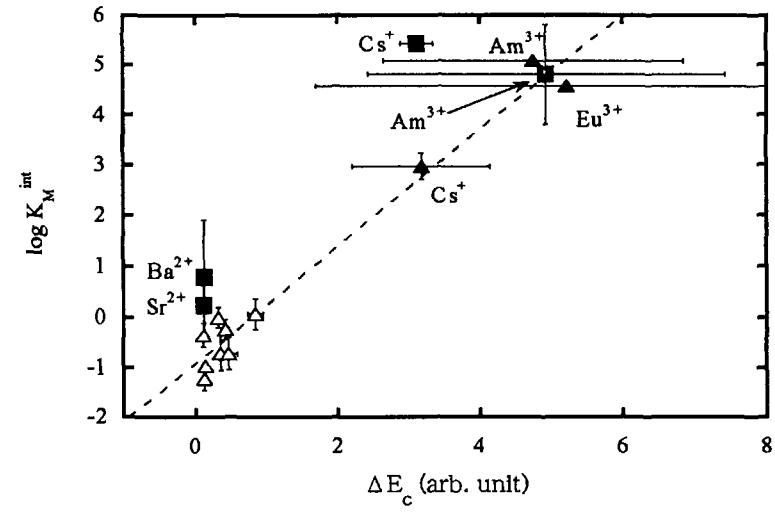

Fig. 4 Intrinsic adsorption equilibrium constant K_M^{int} for quartz as a function of the potential difference ΔE_c. Marks are the analytical data of titration for quartz (△), of K_d measurement for quartz (▲) and of K_d measurement for granite (■). See text for detail.

CONCLUSIONS

Distribution coefficient of cations onto granite was found to increase with increasing pH and with decreasing ionic strength. An electrical double layer model was applied to the analysis of the experimental data, and optimum parameter values were obtained. From the analysis, feldspar was found to play an important role in the adsorption up to pH 10, and biotite to additionally contribute above pH 10. Similarly to the case of quartz, it was found that the parameter values for the electrostatic capacitance and then the dielectric constant in the electrical double layer are much dependent on the distance from the surface because of electrical saturation of water molecules near the surface. Also, the intrinsic adsorption equilibrium constants of the adsorbate cations were found to be simply related with the Coulomb potential differences resulting from their adsorption. Comparing feldspar with quartz, no particular difference was found in the adsorption mechanisms.

ACKNOWLEDGEMENTS

This research was supported by Grant-in-Aid for Scientific Research from the Ministry of Education, Science, Sports and Culture.

REFERENCES

1. J. A. Davis and D. B. Kent, in "Mineral-Water Interface Geochemistry", Reviews in Mineralogy, M. F. Hochella and A. F. White Eds., Mineralogical Society of America, Vol. 23, p. 177(1990).
2. N. Sahai and D. A. Sverjensky, Geochim. Cosmochim. Acta, Vol. 61, p. 2801(1997).
3. J. A. Davis et al., J. Colloid Interface Sci., Vol. 63, p. 480(1978).
4. R. O. James and G. A. Parks, in "Surface Colloid Science", Matijevic, E. Ed., Plenum Press, Vol. 12, p.119(1982).
5. J. C. Westall et al., Tech. Note, Vol. 18, Dept. of Civil. Eng., Mass Inst. Tech., Cambridge, MA(1976).
6. D. S. Brown and J. D. Allison, "MINTEQA1, Equilibrium metal speciation model: A user's manual.", EPA/600/3-87/012, U.S. Environmental Protection Agency, Athens, GA(1987).
7. C. Papelis et al., Tech. Rept., Vol. 306, Dept. of Civil. Eng. Stanford University, Stanford, CA, (1988).
8. R. J. Silva and H. Nitsche, Radiochim. Acta, Vol. 70/71, p. 377(1995).
9. A. Kitamura et al., J. Nucl. Sci. Technol., submitted.
10. J. A. Davis et al., J. Colloid Interface Sci., Vol. 67, p. 90(1978).
11. A. Kitamura et al., J. Nucl. Fuel Cycle Environ., Vol. 4, p. 39(1997).
12. A. Kitamura et al., J. Radioanal. Nucl. Chem., Vol. 239, in press (1999).

13. J. Leja, "Surface Chemistry of Froth Flotation", 3rd Ed., Plenum Press, New York (1982).
14. W. Stumm and J. J. Morgan, "Aquatic Chemistry", 3rd Ed., Wiley Interscience, New York(1996).
15. A. Kitamura et al., J. Nucl. Sci. Technol., Vol. 33, p. 840(1996).
16. C. G. Armistead et al., J. Phys. Chem., Vol. 73, p. 3947(1968).
17. R. J. Silva et al., PNL-SA8571, p. 249(1979).
18. J. Lyklema and J. T. G. Overbeek, J. Colloid Sci., Vol. 16, p. 595(1961).
19. W. Stumm et al., Croat. Chem. Acta, Vol. 42, p. 223(1970).
20. M. Tsukamoto and T. Ohe, Chem. Geol., Vol. 107, p. 29(1993).
21. D. C. Grahame, J. Chem. Phys., Vol. 18, p. 903(1950).